CrystEngComm

Accepted Manuscript

ROYAL SOCIETY OF CHEMISTRY

www.rsc.org/crystengcomm

Positional Isomeric Effect on Structural Variation of Cd(II) Coordination Polymers Based on Flexible Linear/V-Shaped Bipyridyl Benzene Ligands

Lei-Lei Liu,*[a] Cai-Xia Yu,[a] Ya-Ru Li,[a] Jing-Jing Han,[a] Feng-Ji Ma[a] and Lu-Fang Ma*[b]

Received (in XXX, XXX) xxxxx 2014, Accepted xxxxx 2014
First published on the web xxxxx 2014
DOI: 10.1039/c000000x

Self-assembly of Cd(II) ions with five positional isomeric flexible bipyridyl benzene and 2,2'-azodibenzoic acid ligands yield five interesting coordination polymers, $[Cd_2L_2(3\text{-pbpmb})_3]_n$ (**1**), $[Cd_2L_2(2\text{-pbpmb})]_n$ (**2**), $\{[CdL(4\text{-mbpmb})_2]\cdot MeOH\}_n$ (**3**), $\{[Cd_2L_2(3\text{-mbpmb})_3]\cdot 2.5H_2O\}_n$ (**4**) and $[Cd_2Cl_2L(3\text{-obpmb})_2]_n$ (**5**) where H_2L = 2,2'-azodibenzoic acid, 3-pbpmb = 1,4-bis(pyridine-3-ylmethoxy)benzene, 2-pbpmb = 1,4-bis(pyridine-2-ylmethoxy)benzene, 4-mbpmb = 1,3-bis(pyridine-4-ylmethoxy)benzene, 3-mbpmb = 1,3-bis(pyridine-3-ylmethoxy)benzene and 3-obpmb = 1,2-bis(pyridine-3-ylmethoxy)benzene. Their structures have been determined by single-crystal X-ray diffraction analyses, elemental analyses, IR spectra, powder X-ray diffraction (PXRD) and thermogravimetric analyses (TGA). Compound **1** is a 3D architecture constructed by 1D ladder-like $[Cd_4(3\text{-pbpmb})_4]_n$ chains as well as L linkers, and displays an interesting 5-connected net with a $4^6 6^4$ topology. Compound **2** comprises a 3D framework built from 2D wrinkled $[Cd_2L_4]_n$ networks and 2-pbpmb bridges with a 6-connected *pcu* net. Compound **3** bears a 2D network based on $[Cd_2(4\text{-mbpmb})_2]$ building units and 1D $[CdL]_n$ chains. Compound **4** features a 2D network in which the helical $[Cd(3\text{-mbpmb})]_n$ chains are alternately arranged in a right- and left-handed sequence. Compound **5** exhibits a 2D network constructed by the 1D $[Cd_2Cl_2(3\text{-obpmb})_2]_n$ chains and L linkers. The results reveal that the diverse coordination networks of **1**–**5** can be adjusted by the positional isomeric effect of flexible bipyridyl benzene building blocks. Moreover, the luminescent properties of compounds **1**–**5** in the solid state have also been investigated.

Introduction

The design and synthesis of coordination polymers (CPs) have attracted an upsurging research interest not only because of their appealing structural and topological novelty but also owing to their tremendous potential applications in gas storage/adsorption,[1] catalysis,[2] separation,[3] drug delivery[4] and fluorescence.[5] The ultimate aim of coordination chemistry is to control the structures of target products and investigate the relationships between structures and properties.[6] Accordingly, many intriguing topological types and associated interesting properties have been investigated in depth.[7] However, how to rational design and synthesis of CPs with desired structures and properties is still a long-term challenge. The structural diversity of such materials is usually influenced by many factors, such as metal ions, metal/ligand ratios, the nature of organic ligands, pH value and counter anion.[8-10] Without a doubt, among these factors, the selection of appropriate ligands is a very important one because they are highly tunable, and even small changes can result in a remarkable diversity of both architectures and properties.[11] With this understanding, one crucial aim of this work is to explore the essential factors of positional isomeric ligands for regulating the structural assembly, which may provide further insights in designing new functional crystalline materials.[12]

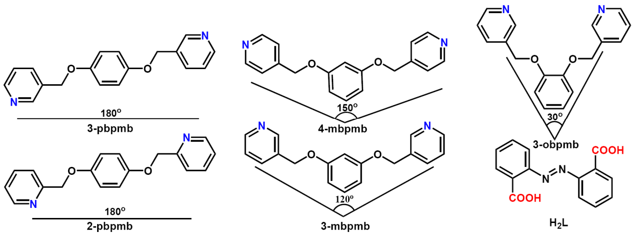

Scheme 1 Structures of the organic ligands used in this work.

Flexibility is critical for the construction of a coordination polymer because the shape, symmetry and length of a ligand can be affected by its flexibility.[9a-b,12e] Generally, the rigid ligands are prone to form coordination polymers with expected structures. However, the structures of coordination polymers constructed from flexible ligands are not easy to predict since the flexible ligands can freely rotate and adopt a variety of conformations according to the restrictions imposed by the coordination geometry of the metal ions. As a result, an increasing number of

---

[a] *College of Chemistry and Chemical Engineering, Anyang Normal University, Anyang 455000, Henan, P. R. China. E-mail: liuleileimail@163.com*
[b] *College of Chemistry and Chemical Engineering, Luoyang Normal University, Luoyang 471022, Henan, P. R. China. E-mail: mazhuxp@126.com*

† Electronic supplementary information (ESI) available: PXRD patterns, TGA curves and additional figures for **1-5**. CCDC reference numbers: 992498–992502. For crystallographic data in CIF or other electronic format see DOI: 10.1039/c000000x

interesting CPs incorporating flexible ligands with d^{10} metal ions have been reported recently.[10a-b,11c-d]

Flexible bipyridyl benzene ligands contain rigid benzene ring piece and two freely rotating pyridyl arms combined by intervening methoxy groups (Scheme 1). The pyridyl arms can freely twist around the –O–CH_2– group to meet the requirements of the coordination arrangements of metal atoms in the assembly process, which can easily produce unique structural motifs with beautiful aesthetics and useful functional properties.[13-15] In addition, the different positions of the pyridyl N atoms and methoxyl O atoms in the positional isomeric ligands (Scheme 1) maybe benefit the formation of different topological structures. Moreover, a systematic study of the positional isomeric effect of such bipyridyl ligands on the structural assemblies with d^{10} metal ions is relatively rare. Hence, systematic research on the coordination chemistry of such bipyridyl ligands is necessary for constructing novel framework structures and understanding topology control. We were curious to know whether this was simply a serendipitous event or a more general reaction that would apply to other structurally related ligands.

With this in mind, here, we present the syntheses and crystal structures of five Cd(II) coordination polymers built from such five isomeric tectons and 2,2'-azodibenzoic acid (H_2L) ligand under solvothermal conditions, including $[Cd_2L_2(3\text{-pbpmb})_3]_n$ (**1**), $[Cd_2L_2(2\text{-pbpmb})]_n$ (**2**), $\{[CdL(4\text{-mbpmb})_2]\cdot MeOH\}_n$ (**3**), $\{[Cd_2L_2(3\text{-mbpmb})_3]\cdot 2.5H_2O\}_n$ (**4**) and $[Cd_2Cl_2L(3\text{-obpmb})_2]_n$ (**5**), which exhibit a systematic variation of architectures from 2D networks to 3D frameworks. And the L ligand in **1**–**5** displays varied coordination modes (Scheme 2). Furthermore, the thermal and fluorescence properties of these compounds are also discussed in detail.

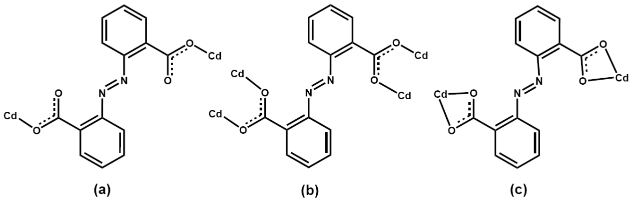

Scheme 2 Diverse coordination types of L ligands in compounds **1**−**5**.

Experimental

Materials and physical measurements

H_2L, 3-pbpmb, 2-pbpmb, 4-mbpmb and 3-obpmb were prepared according to the previously reported procedure.[16] All other chemicals and reagents were obtained from commercial sources and used as received. IR spectra were recorded with a Varian 800 FT-IR spectrometer as KBr disks (4000-400 cm^{-1}). ^1H NMR and ^{13}C NMR spectra were recorded at ambient temperature with a Bruker Avance III-400 spectrometer. The ^1H NMR chemical shifts are reported relative to TMS in $CDCl_3$. The ^{13}C NMR chemical shifts were referenced to the deuterated $CDCl_3$ signal. The elemental analyses for C, H, and N were performed on an EA1110 CHNS elemental analyzer. Powder X-ray diffraction (PXRD) was performed using a PANalytical X'Pert PRO MPD system and Bruker Ultima III X-ray diffractometer. Luminescent spectra were recorded with a JASCO FP-8600 fluorescence spectrophotometer. Thermal analysis were performed with a Netzsch STA-409 PC thermogravimetric analyzer at a heating rate of 20 °C min^{-1} and a flow rate of 20 cm^3 min^{-1} (N_2).

Preparation of 1,3-bis(pyridine-3-ylmethoxy)benzene (3-mbpmb)

A mixture of 1,3-dihydroxybenzene (1.00 g, 9.08 mmol) and K_2CO_3 (12.53 g, 90.80 mmol) in DMF (17 mL) was combined with a mixture of 3-(chloromethyl)pyridine hydrochloride (3.57 g, 21.79 mmol) and KI (0.53 g, 3.20 mmol) in DMF (5 mL). The reaction solution was stirred at room temperature for 85 h. The resulting solution was added to 60 mL H_2O and 100 mL $CHCl_3$, and the mixture was further stirred at room temperature for 1 h. Then the mixture was extracted by $CHCl_3$ (3 × 20 mL). The combined organic layers were washed with water and saturated NaCl, respectively, dried with anhydrous Na_2SO_4, and the solvent was removed in vacuo to yield the crude product. Purification by silica gel chromatography using 200~300 mesh ZCX II eluted by ethyl acetate gave compound 3-mbpmb (1.81 g, 68%). Anal. Calcd. for $C_{18}H_{16}N_2O_2$: C, 73.95; H, 5.52; N, 9.58. Found: C, 73.75; H, 5.69; N, 9.75. IR (KBr disc): 3446 (m), 3437 (w), 3025 (w), 2927 (w), 2856 (w), 1593 (s), 1578 (s), 1506 (s), 1475 (w), 1457 (m), 1429 (m), 1384 (m), 1328 (w), 1258 (s), 1215 (s), 1124 (m), 1009 (s), 924 (w), 865 (m), 795 (m), 728 (m), 712 (m), 619 (w) cm^{-1}. ^1H NMR (400 MHz, $CDCl_3$): δ 8.68 (s, 2H), 8.59 (t, 2H), 7.77 (d, 2H), 7.32 (m, 2H), 7.22 (m, 1H), 6.62 (d, 3H), 5.06 (s, 4H, CH_2). ^{13}C NMR (400 MHz, $CDCl_3$): δ 159.68, 149.97, 148.98, 135.27, 132.41, 130.21, 123.52, 107.66, 102.39, 67.62.

Preparation of compounds 1–5

$[Cd_2L_2(3\text{-pbpmb})_3]_n$ (1). A 10 mL Pyrex glass tube was loaded with $Cd(OAc)_2\cdot 2H_2O$ (11 mg, 0.04 mmol), H_2L (6 mg, 0.02 mmol), 3-pbpmb (6 mg, 0.02 mmol), 0.01 M HCl (0.2 mL) and 4 mL of MeOH/H_2O (1:1 V/V). The tube was then sealed and heated in an oven to 170 °C for four days, and then cooled to ambient temperature at a rate of 5 °C h^{-1}. The yellow block crystals of **1** were formed four days later, which were collected and washed thoroughly with MeOH and dried in air. Yield: 8 mg (49%, based on H_2L). Anal. Calcd. for $C_{82}H_{64}N_{10}Cd_2O_{14}$: C, 60.12; H, 3.94; N, 8.55. Found: C, 60.50; H, 3.77; N, 8.19. IR (KBr disc): 3438 (m), 3426 (w), 3016 (w), 2917 (w), 2816 (w), 1595 (s), 1561 (s), 1506 (s), 1443 (w), 1401 (m), 1283 (w), 1223 (m), 1046 (m), 957 (w), 857 (m), 826 (m), 771 (m), 731 (w), 704 (m), 662 (m), 558 (w) cm^{-1}.

$[Cd_2L_2(2\text{-pbpmb})]_n$ (2). Compound **2** (orange blocks) was prepared in the same way as **1**, except using 2-pbpmb instead of 3-pbpmb. Yield: 6 mg (57%, based on H_2L). Anal. Calcd. for $C_{46}H_{32}N_6Cd_2O_{10}$: C, 52.44; H, 3.06; N, 7.98. Found: C, 52.55; H, 3.38; N, 7.61. IR (KBr disc): 3366 (w), 3411 (w), 2915 (w), 2975 (w), 1633 (s), 1592 (s), 1574 (m), 1505 (s), 1458 (w), 1409 (s), 1316 (w), 1244 (w), 1201 (s), 1098 (w), 1041 (s), 859 (m), 824 (m), 774 (m), 754 (m), 717 (m), 661 (m), 556 (w) cm^{-1}.

$\{[CdL(4\text{-mbpmb})_2]\cdot MeOH\}_n$ (3). Compound **3** (orange blocks) was prepared in the same way as **1**, except using 4-mbpmb instead of 3-pbpmb. Yield: 6 mg (30%, based on H_2L). Anal. Calcd. for $C_{51}H_{44}N_6CdO_9$: C, 61.42; H, 4.45; N, 8.43. Found: C, 61.72; H, 4.72; N, 8.21. IR (KBr disc): 3435 (w), 2974 (w), 2926 (w), 1603 (s), 1586 (s), 1562 (m), 1507 (s), 1458 (w), 1433 (w), 1386 (m), 1229 (m), 1045 (s), 855 (w), 834 (w), 777 (m), 706 (m), 645 (w), 529 (w) cm^{-1}.

{[Cd$_2$L$_2$(3-mbpmb)$_3$]·2.5H$_2$O}$_n$ (4). Compound **4** (orange blocks) was prepared in the same way as **1**, except using 3-mbpmb instead of 3-pbpmb. Yield: 7 mg (42%, based on H$_2$L). Anal. Calcd. for $C_{82}H_{69}N_{10}Cd_2O_{16.5}$: C, 58.51; H, 4.13; N, 8.32. Found: C, 58.36; H, 4.55; N, 8.25. IR (KBr disc): 3436 (m), 2974 (w), 2926 (w), 1608 (s), 1594 (s), 1507 (m), 1443 (w), 1397 (s), 1286 (w), 1200 (w), 1097 (w), 1047 (m), 857 (w), 825 (w), 771 (m), 729 (w), 662 (w), 560 (w) cm^{-1}.

[Cd$_2$Cl$_2$L(3-obpmb)$_2$]$_n$ (5). Compound **5** (yellow blocks) was prepared in the same way as **1**, except using 3-obpmb instead of 3-pbpmb. Yield: 5 mg (22%, based on H$_2$L). Anal. Calcd. for $C_{50}H_{40}N_6Cl_2Cd_2O_8$: C, 52.28; H, 3.51; N, 7.32. Found: C, 52.56; H, 3.75; N, 7.03. IR (KBr disc): 3528 (w), 3016 (w), 2931 (w), 2856 (w), 1594 (m), 1575 (s), 1544 (m), 1505 (s), 1461 (w), 1438 (w), 1399 (s), 1328 (w), 1258 (s), 1216 (m), 1125 (m), 1015 (m), 865 (m), 791 (w), 774 (m), 735 (m), 702 (m), 662 (m), 585 (w) cm^{-1}.

Table 1 Summary of Crystallographic Data for **1**–**5**

Compound	1	2	3	4	5
Empirical Formula	$C_{41}H_{32}CdN_5O_7$	$C_{23}H_{16}CdN_3O_5$	$C_{51}H_{40}CdN_6O_9$	$C_{164}H_{138}Cd_4N_{20}O_{33}$	$C_{25}H_{20}CdClN_3O_4$
Formula Weight	819.12	526.79	993.29	3366.54	574.29
Crystal System	triclinic	triclinic	triclinic	monoclinic	triclinic
Space Group	$P\bar{1}$	$P\bar{1}$	$P\bar{1}$	$P2_1/c$	$P\bar{1}$
a (Å)	9.820(2)	9.976(2)	9.809(2)	20.660(4)	10.056(2)
b (Å)	11.519(2)	10.462(2)	15.607(3)	20.899(4)	10.955(2)
c (Å)	16.954(3)	10.933(2)	16.604(3)	18.580(4)	11.676(2)
α (°)	101.25(3)	81.98(3)	81.76(3)	90	113.00(3)
β (°)	97.92(3)	67.17(3)	88.16(3)	102.46(3)	97.99(3)
γ (°)	96.46(3)	84.87(3)	72.57(3)	90	92.39(3)
V (Å^3)	1843.6(6)	1040.6(4)	2400.1(8)	7833(3)	1165.9(4)
Z	2	2	2	2	2
T (K)	296(2)	296(2)	296(2)	296(2)	296(2)
ρ_{calc} (g/cm^3)	1.476	1.681	1.374	1.427	1.636
F(000)	834.0	526.0	1016.0	3436.0	576.0
μ (MoKα, mm^{-1})	0.651	1.091	0.517	0.617	1.089
Total reflections	13890	7675	16512	58647	8053
Unique reflections	6473 (R_{int} = 0.0403)	3646 (R_{int} = 0.0134)	8396 (R_{int} = 0.0357)	13776 (R_{int} = 0.0512)	4075 (R_{int} = 0.0200)
No. of observations	5330	3492	7720	9930	3653
No. of parameters	487	289	622	1009	207
$R_1{}^a$	0.0421	0.0177	0.0339	0.0354	0.0236
$wR_2{}^b$	0.1155	0.0488	0.1080	0.0920	0.0531
GOF^c	1.065	1.067	1.080	1.016	1.055

^{a} $R_1 = \Sigma||F_o|-|F_c|/\Sigma|F_o|$. ^{b} $wR_2 = \{\Sigma w(F_o^2-F_c^2)^2/\Sigma w(F_o^2)^2\}^{1/2}$. ^{c} GOF = $\{\Sigma w(F_o^2-F_c^2)^2/(n-p)\}^{1/2}$, where n = number of reflections and p = total numbers of parameters refined.

X-Ray data collection and structure determination

Single crystals of **1**–**5** were obtained directly from the above preparations. All measurements were made on a Bruker Smart Apex-II CCD area detector by using graphite monochromated Mo Kα (λ = 0.071073 nm). These crystals were mounted on glass fibers at 296 K for **1**–**5**. Diffraction data were collected at f and ω modes with a detector distance of 35 mm to the crystals. Cell parameters were refined by using the program Bruker *SAINT*. The collected data were reduced by using the program Bruker *SAINT* A, and the absorption corrections (multi-scan) were applied. The reflection data were also corrected for Lorentz and polarization effects. The crystal structures of **1**–**5** were solved by direct method refined on F^2 by full-matrix least-squares techniques with the SHELXTL-97 program.[17a] Hydrogen atoms of the MeOH solvent molecules in **3** (O9, O10, C51, C52) were not located. All other H atoms in **1**–**5** were placed in geometrically idealized positions and constrained to ride on their parent atoms. The site occupation factors for O9-O10, C51-C52 atoms in **3** and O3W, O4W atoms in **4** were fixed at 0.5 and 0.25, respectively.[17b] A summary of the key crystallographic information for **1**–**5** is tabulated in Table 1 and their selected bond lengths as well as angles are given in Table 2 and Table S1.

Results and discussion

Synthetic and spectral aspects

In all solvothermal reactions reported here, the molar ratio of $Cd(OAc)_2\cdot2H_2O$ to H_2L and N-donor ligands was kept at 2 : 1 : 1. Reactions of $Cd(OAc)_2\cdot2H_2O$ with H_2L and corresponding N-donor ligands at 170 °C for four days produced crystals of **1** (yellow, 49% yield), **2** (orange, 57% yield), **3** (orange, 30% yield), **4** (orange, 42% yield) and **5** (yellow, 22% yield), respectively. When the reactions were carried out at lower temperatures (150 °C), the same products of **1**–**5** with relatively lower yields were obtained. Even more, decreasing the temperature to 120 °C or 90 °C, only orange precipitates were isolated and their PXRD patterns were inconsistent with those of **1**–**5**.

Compounds **1**–**5** were stable towards oxygen and moisture, and almost insoluble in common organic solvents. Their elemental analysis was consistent with the chemical formulas of **1**–**5**. In order to check the phase purity of **1**–**5**, the powder X-ray diffraction (PXRD) patterns were measured at room temperature (Fig. S1–S2, ESI†). The IR spectra of **1**–**5** showed peaks in the range of 1594−1633 cm^{-1} and 1397–1433 cm^{-1}, suggesting they all contain coordinated carboxylic groups.[18] The peaks at 825–865 cm^{-1}, and peaks in the range of 645–662 cm^{-1} mean the existence of pyridyl groups in the compounds of **1**–**5**.[19] The identities of **1**–**5** were finally confirmed by single-crystal diffraction analysis.

Crystal structure of 1

Compound **1** crystallizes in the triclinic space group $P\bar{1}$, and its asymmetric unit contains one Cd atom, one and a half 3-pbpmb ligands, two halves of L ligands. As shown in Fig. 1a, each Cd1 atom is coordinated by three N atoms (Cd1–N5A = 2.345(3) Å, Cd1–N4 = 2.368(3) Å, Cd1–N3 = 2.384(3) Å) of three 3-pbpmb ligands, two O atoms (Cd1–O3 = 2.367(3) Å, Cd1–O4 = 2.472(3) Å) of chelating carboxylate groups from one L ligand, one O atom (Cd1–O1 = 2.244(3) Å) of bridging carboxylate groups from the second L ligand to furnish a distorted octahedral coordination geometry. The mean Cd–N bond length (2.365(6) Å) is little longer than that of in $\{[Cd(HL5)_2(biim\text{-}4)_{1.5}]\cdot H_2O\}_n$. (2.302(5) Å, H_2L5 = 5-chlorosalicylic acid, biim-4 = 1,1'-(1,4-butanediyl)bis(imidazole)).[20] While the mean Cd–O bond length (2.361(6) Å) is little shorter than that observed in $\{[Cd(HL5)_2(biim\text{-}4)_{1.5}]\cdot H_2O\}_n$. (2.446(6) Å).[20] The carboxylate groups of L in **1** display μ_1-η^1:η^0 and μ_1-η^1:η^1 coordination modes, respectively (Schemes 2a and 2c). Cd1 atom and its own three symmetry-related atoms are bridged by N atoms from four 3-pbpmb ligands to give a rhombic-like $[Cd_4(3\text{-pbpmb})_4]$ unit (15.44 × 18.38 $Å^2$, Fig. 1b). Then, such units are interlinked together through sharing the 3-pbpmb ligands to generate a 1D ladder-like chain extending along the *c* axis (Fig. 1b). Each 1D chain is connected to its adjacent ones *via* carboxylate groups from L ligands (pink) to form a 2D network extending along the *ac* plane (Fig. 1c). Each 2D network is further bridged by carboxylate groups form second L ligands to afford a 3D structure (Fig. 1d). From the viewpoint of topology,[21] if the Cd(II) centres are considered as nodes, the 3-pbpmb and L ligands are considered as linkers, the whole structure of **1** can be specified by a Schläfli symbol of $4^6\cdot6^4$ (Fig. 1e). Comparison of the previously reported complexes,[14c,15b] $[Ag(3\text{-pbpmb})(NO_3)\cdot H_2O]$, $[Zn(3\text{-pbpmb})(bdc)(H_2O)]_n$ and $[Cd(3\text{-pbpmb})(bbdc)(H_2O)(DMF)]_n$, the 3-pbpmb were bridged by Ag/Zn/Cd atoms affording the 1D zig-zag or helical chains. These results indicated that the species of metal ions did work on the final structures.

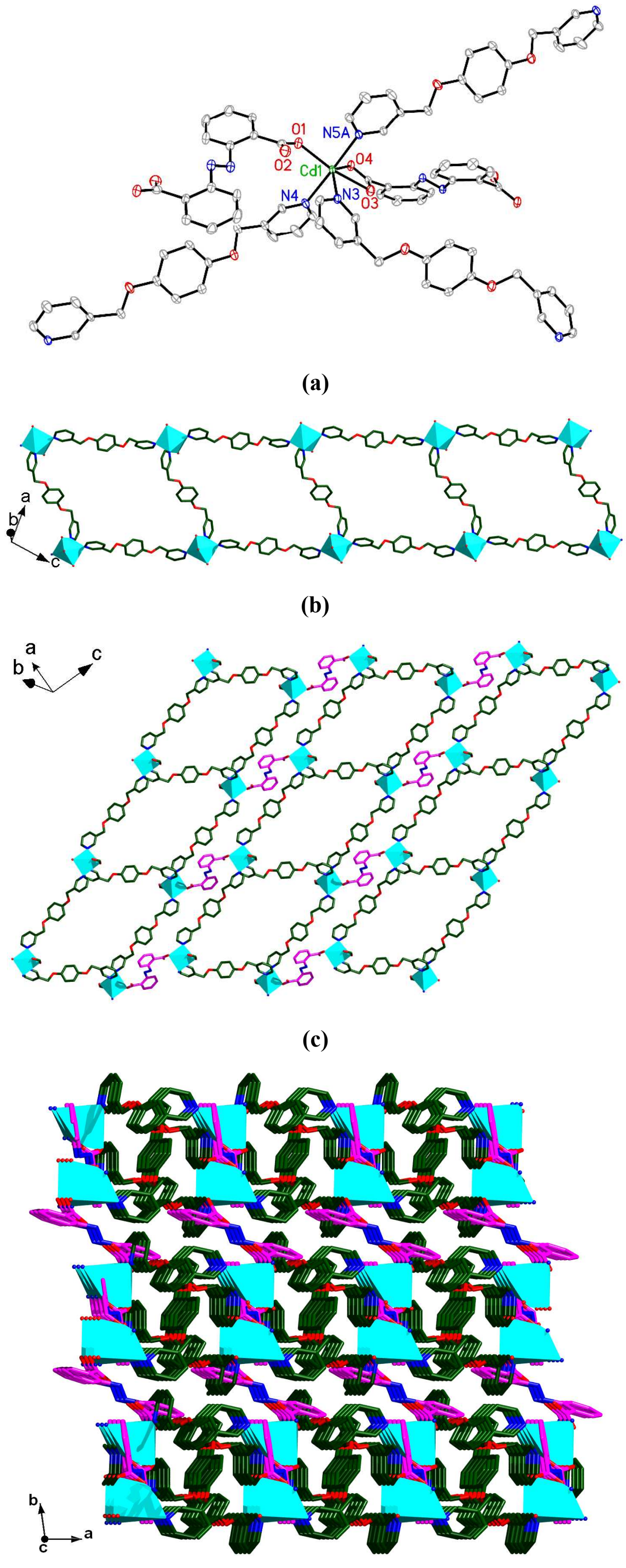

(a)

(b)

(c)

(d)

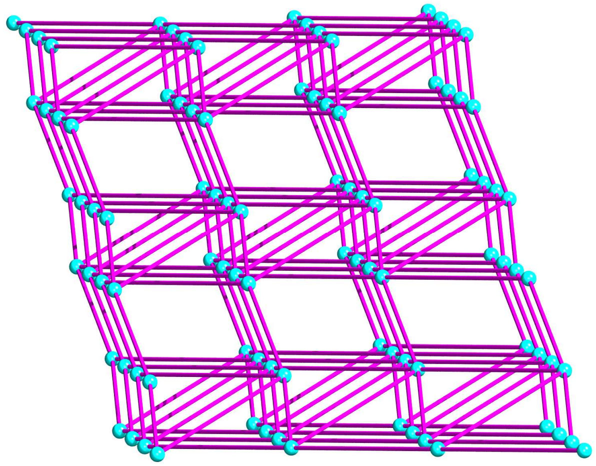

(e)

Fig. 1 (a) View of the coordination environments of Cd center in **1** with labeling schemes. Symmetry codes: (A) $x + 1, y, z + 1$. (b) View of a 1D ladder-like chain in **1** extending along the *ac* plane. (c) View of a 2D network in **1** extending along the *bc* plane. (d) View of a 3D structure in **1** looking down the *c* axis. (e) Schematic view of a $4^6 \cdot 6^4$ topological net of **1**. Atom color codes: Cd, cyan polyhedrons; O, red; N, blue; C, dark green and pink. All H atoms are omitted for clarity.

Crystal structure of 2

Compound **2** crystallizes in the triclinic space group $P\bar{1}$, and its asymmetric unit contains one Cd atom, a half 2-pbpmb ligand, two halves of L ligands. Cd1 atom adopts a pyramidal coordination geometry and is five-coordinated by four O atoms of four bridging carboxylate groups from four L ligands and one N atom of 2-pbpmb ligand (Fig. 2a), which is less reported in the Cd(II)-based compounds.[22] The Cd–N bond length is 2.2670(17) Å, and the Cd–O bond lengths range from 2.1886(16) to 2.2951(17) Å, which are in the normal range. Notably, a weak interaction (2.8436(17) Å) exists between Cd1 and O5 from 2-pbpmb ligand (Fig. 2a). In contrast, the carboxylate groups of L in **2** only adopt μ_2-η^1:η^1 coordination mode (Scheme 2b). Cd1 atom and its symmetry-related Cd1A atom are bridged by four carboxylate groups to generate a paddle-wheel $[Cd_2(\mu_2\text{-}CO_2)_4]$ unit. The Cd atoms are further surrounded by N atoms to produce a rare dinuclear $[Cd_2N_2(\mu_2\text{-}CO_2)_4]$ unit (Fig. 2b). The Cd···Cd separation in this dinuclear unit is 3.250 Å, which is shorter than that found in related $[Cd_2P_2(\mu_2\text{-}CO_2)_4]$ (3.452 Å) and $[Cd_2Cl_2(\mu_2\text{-}CO_2)_4]$ (3.361 Å) units.[22] Each paddle-wheel $[Cd_2N_2(\mu_2\text{-}CO_2)_4]$ unit serves as a four-fold node, which links its four equivalent ones *via* sharing four L ligands to form a 2D wrinkled network extending along the *bc* plane (Fig. 2c). Furthermore, the 2-pbpmb ligands are employed as linkers (pink) to bridge the 2D networks to form a 3D framework (Fig. 2d). Topologically, the overall structure of **2** can be described as a *pcu* net with the 6-connected $4^{12}6^3$ topology (Fig. 2e). While in the previously reported complexes,[13c,14a-14b] $Ag_2(2\text{-pbpmb})_2(NO_3)_2$, $[Ag(2\text{-pbpmb})(NO_3)]_n$ $\{[Ag(2\text{-pbpmb})]CF_3SO_3\}_n$ and $\{[Ag(2\text{-pbpmb})_2]CF_3SO_3\}_n$, which showed 0D cage-like structure, 1D chain and 2D network, respectively.

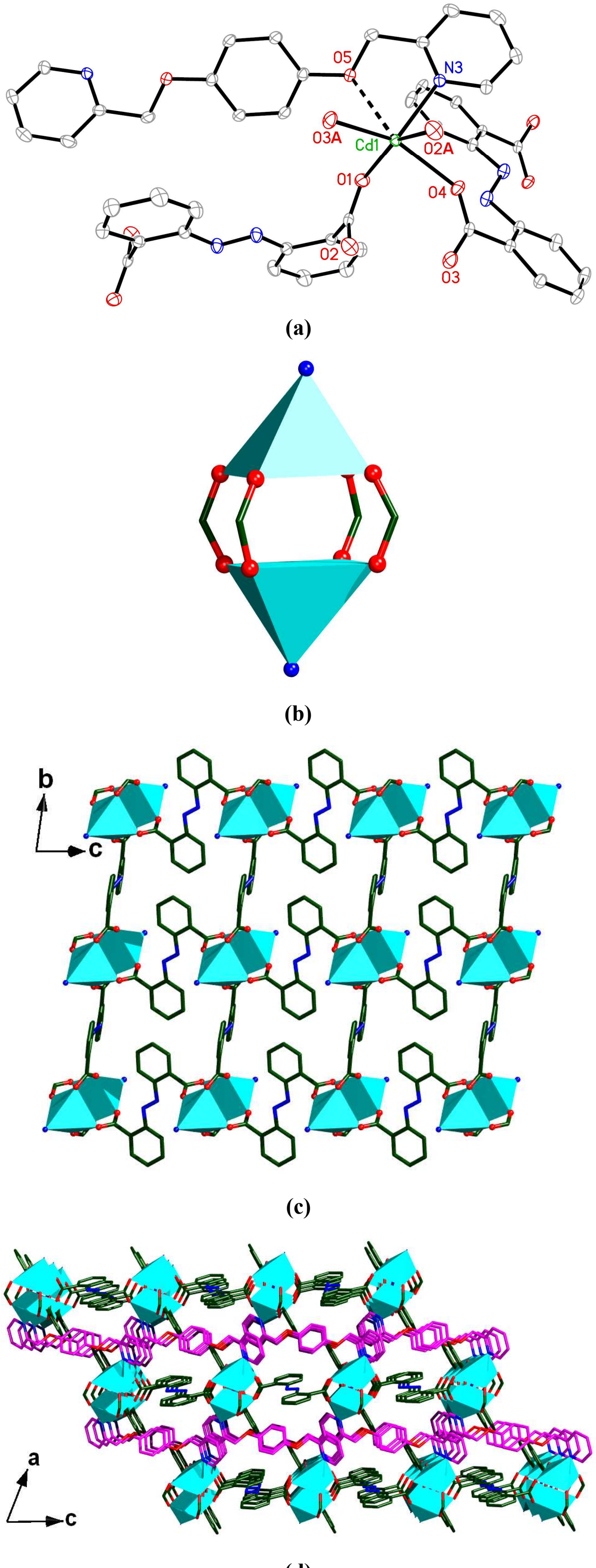

(a)

(b)

(c)

(d)

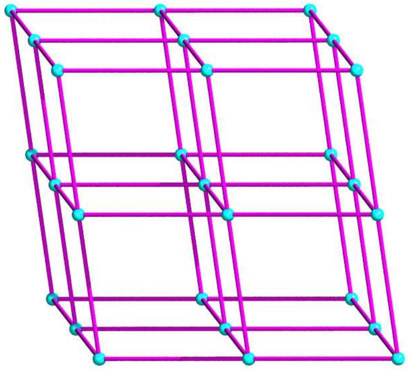

(e)

Fig. 2 (a) View of the coordination environments of Cd center in **2** with labeling schemes. Symmetry codes: (A) $1 - x, 1 - y, 1 - z$. (b) View of one dinuclear $[Cd_2N_2(\mu_2\text{-}CO_2)_4]$ unit of **2**. (c) View of a wrinkled 2D network in **2** extending along the *bc* plane. (d) View of a 3D framework of **2** looking down the *b* axis. (e) Schematic view of a $4^{12}6^3$ topological net of **2**. Atom color codes: Cd, cyan polyhedrons; O, red; N, blue; C, dark green and pink. All H atoms are omitted for clarity.

Crystal structure of 3

Compound **3** crystallizes in the triclinic space group $P\bar{1}$, and its asymmetric unit contains one Cd atom, two halves of L ligands, two 4-mbpmb ligands and two halves of MeOH solvent molecules. Cd1 atom is coordinated by four O (O1, O2, O3, O4) atoms of two chelating carboxylate groups from two different L ligands, three N (N3, N5, N6A) atoms from three 4-mbpmb ligands to furnish a distorted pentagonal bipyramidal coordination geometry (Fig. 3a). The mean Cd–O bond length (2.441(3) Å) is comparable with a related structure of $\{[Cd(CPE)(btbp)_{1.5}]\cdot 4H_2O\}_n$ (2.452(5) Å, H_2CPE = (3-carboxyl-phenyl)-(4-(2′-carboxyl-phenyl)-benzyl) ether, btbp = 4,4′-bis(1,2,4-triazol-1-ylmethyl)biphenyl)), while the average Cd–N bond length (2.369(3) Å) is longer than that observed in $\{[Cd(CPE)(btbp)_{1.5}]\cdot 4H_2O\}_n$ (2.335(5) Å).[23] Cd1 atom and its own symmetry-related atoms are linked by N atoms from two 4-mbpmb ligands to give a metallocyclic $[Cd_2(\text{4-mbpmb})_2]$ unit with the adjacent Cd···Cd distance of 16.444 Å (Fig. 3b). The carboxylate groups of L ligands in **3** only adopt $\mu_1\text{-}\eta^1{:}\eta^1$ coordination mode (Scheme 2c) to link the Cd centers affording a 1D $[CdL]_n$ chain (Fig. S3). The 1D $[CdL]_n$ chain and $[Cd_2(\text{4-mbpmb})_2]$ unit are braided together through sharing Cd atoms to produce a 2D network (Fig. 3c). Each 2D network is further interconnected with neighbouring ones *via* intermolecular hydrogen bond between the methylene of 4-mbpmb ligand and a CO_2^- group in another network (C27–H27A···O1, 3.413 Å) to form a 3D framework with 1D channels (11.32 × 19.01 Å^2) extending along the *ac* plane (Fig. 3d). This structure is also stabilized by *π*–*π* stacking interactions between the pyridine (atoms N4/C28–C32) rings from 4-mbpmb ligands and benzene (atoms C2–C7) rings from L ligands, with a centroid-to-centroid distance of 3.653 Å (Fig. 3d). Calculation of the void volume for **3** by PLATON analysis revealed a pore-accessible volume of 15.1% with respect to the whole unit cell volume (363.4. Å^3 out of the 2400.0 Å^3 per unit cell volume), and the solvent MeOH molecules locate in the free void spaces of the channels (Fig. 3d).

Even though, these channels are still filled by mutual interpenetration of two independent equivalent frameworks, generating a 2-fold interpenetrating 3D architecture (Fig. 3e). If the Cd(II) centres are considered as nodes and the 4-mbpmb, L ligands and hydrogen bonds are considered as linkers, the structure of **3** can be specified as a 6^6 diamondoid network (Fig. 3e). Comparing with the previous reports,[13b] 4-mbpmb respectively reacted with $Zn^{II}/Cd^{II}/Hg^{II}$ salts and obtained three corresponding coordination polymers $\{[Zn/Cd/Hg(\text{4-mbpmb})(H_2O)(NO_3)_2]\cdot(\text{4-mbpmb})\}_n$, which only displayed 1D wavelike chains. This result suggested that the auxiliary ligand H_2L played a very important role on the final polymer.

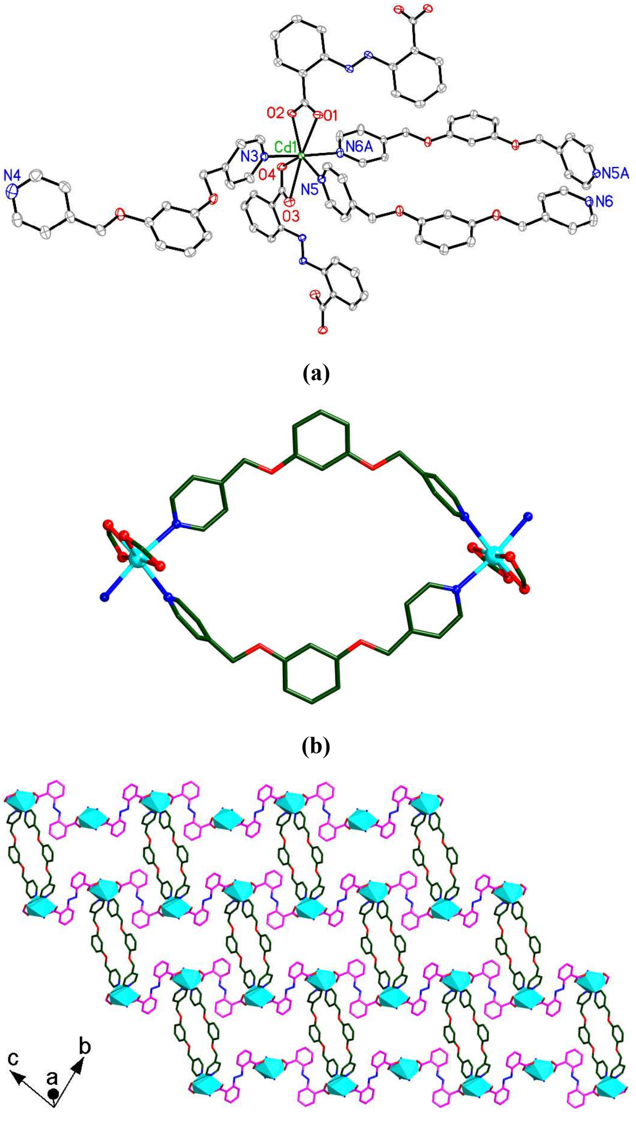

(a)

(b)

(c)

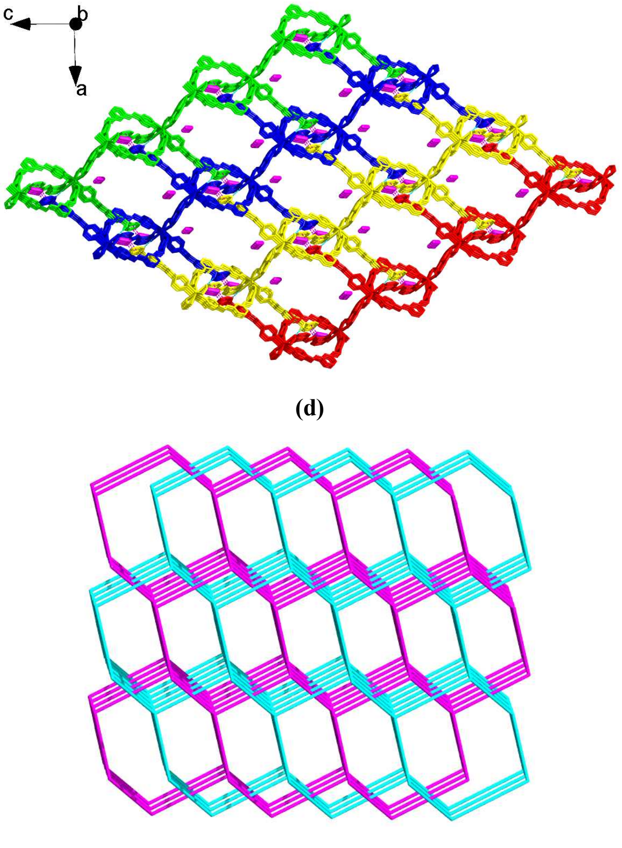

(d)

(e)

Fig. 3 (a) View of the coordination environments of Cd1 center in **3** with labeling schemes. Symmetry codes: (A) 1 − *x*, 2 − *y*, 2 − *z*. (b) View of one [Cd_2(4-mbpmb)$_2$] metallocyclic unit of **3**. (c) View of a 2D network in **3** extending along the *bc* plane. (d) View of a 3D hydrogen-bonded framework in **3** looking down the *b* axis. Cyan dashed lines represent the hydrogen-bonded interactions. Pink dashed lines represent the *π*–*π* interactions. Pink sticks represent MeOH molecules. (e) View of the two-fold interpenetration model in **3**. Each single net represents a topology with a Schläfli symbol 6^6. Atom color codes: Cd, cyan polyhedrons; O, red; N, blue; C, dark green and pink. All H atoms except those related to H-bonding interactions and uncoordinated MeOH molecules are omitted for clarity.

Crystal structure of 4

Compound **4** crystallizes in the monoclinic space group $P2_1/c$, and its asymmetric unit contains two crystallographically unique Cd atoms, two L ligands, three 3-mbpmb ligands, two H_2O solvent molecules and two quarters of H_2O solvent molecules. The coordination environment of Cd(II) in **4** is similar with that of in **3**. Cd1 and Cd2 atoms both adopt the bipyramidal coordination geometry and are seven-coordinated by four O atoms of two chelating carboxylate groups from two different L ligands, three N atoms from three 3-mbpmb ligands (Fig. 4a-4b). The mean Cd–O bond length (2.420(3) Å) is little shorter in comparison with that of in **3** (2.441(3) Å), whereas the average Cd–N bond length (2.388(3) Å) is longer than that of in **3** (2.369(3) Å). Similar to that in **3**, the carboxylate groups of L ligands in **4** also display μ_1-η^1:η^1 coordination mode (Scheme 2c). As shown in Fig. 4c, Cd(II) ions are bridged by 3-mbpmb ligands generating a 1D helical [Cd(3-mbpmb)]$_n$ (the right-handed helix) chain along the *b* axis. And the Cd centers in this 1D helical chain are further coordinated by carboxylate groups from L ligands to stabilize this structure (Fig. S4a). It is interesting that the 1D helical [Cd(3-mbpmb)]$_n$ chains are linked together through N atoms from second 3-mbpmb ligands (green) to form a 2D network extending along *ab* plane (Fig. 4d). Notably, the neighbouring helical chains exhibit two kinds of helix (the left-handed helix and the right-handed helix, respectively) (Fig. 4d). Furthermore, the 2D networks were linked *via* *π*–*π* interactions (3.646 Å) between pyridine (atoms N7/C51–C55) and benzene (atoms C39–C44) rings from 3-mbpmb ligands, resulting in a 3D supramolecular structure (Fig. S4b). And the H_2O solvent molecules were located in the layers of 2D networks through the O–H···O and O–H···N hydrogen-bonding interactions (Fig. S4c). The overall structure of **4** can be simplified into a 6^3 topological net (Fig. 4e).

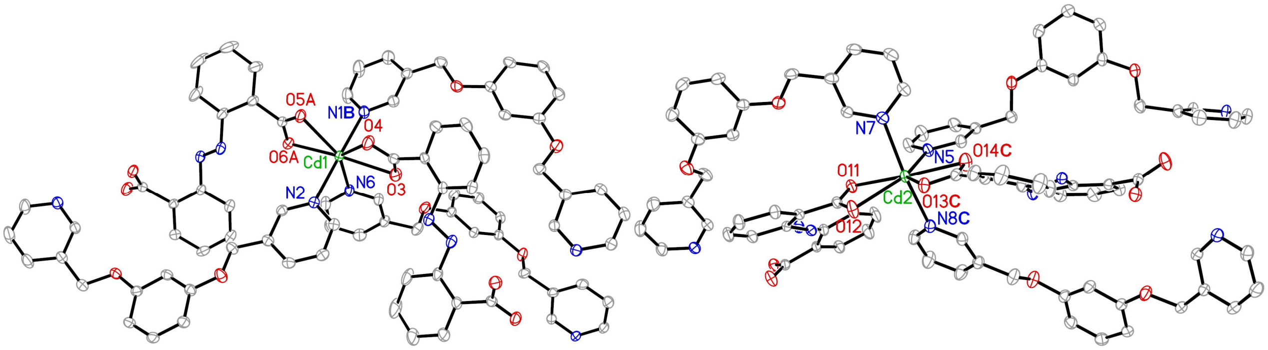

(a) (b)

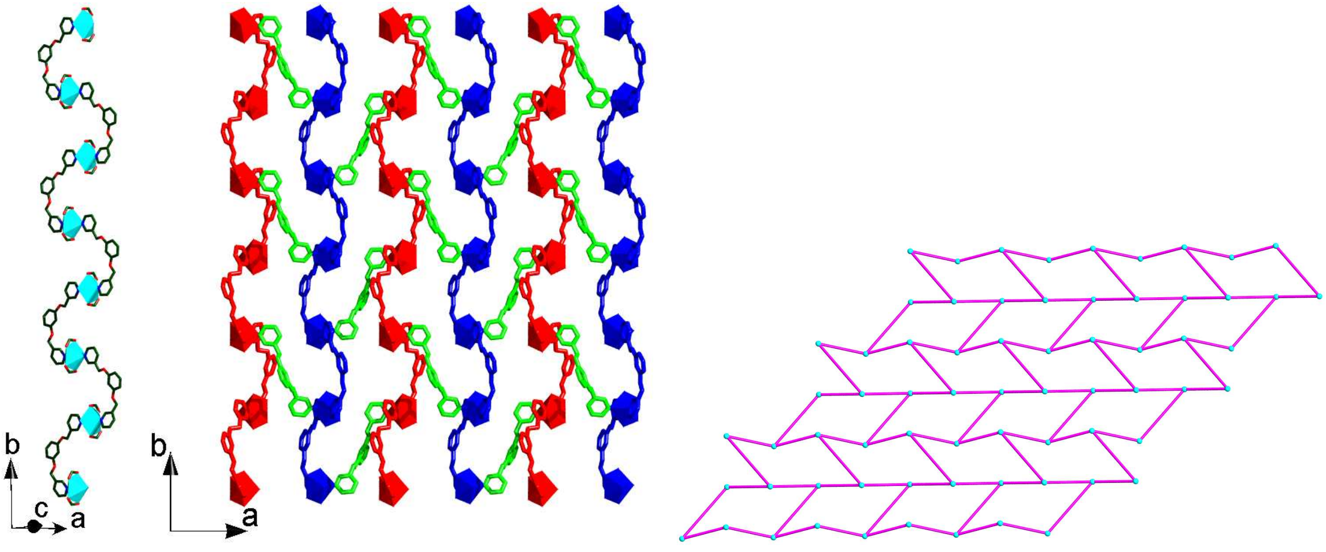

(c) (d) (e)

Fig. 4 (a)–(b) View of the coordination environments of Cd centers in **4** with labeling schemes. Symmetry codes: (A) $1 - x$, $-1/2 + y$, $3/2 - z$; (B) $1 - x$, $1/2 + y$, $3/2 - z$; (C) $2 - x$, $1/2 + y$, $3/2 - z$. (c) View of a 1D helical $[Cd(3\text{-mbpmb})]_n$ chain in **4** extending along the *b* axis. (d) View of a 2D network in **4** extending along the *ab* plane. (e) View of a topological structure of **4**. Atom color codes: Cd, cyan polyhedrons; O, red; N, blue; C, dark green. All H atoms and L ligands are omitted for clarity.

Crystal structure of 5

Compound **5** crystallizes in the triclinic space group $P\bar{1}$, and its asymmetric unit contains one Cd atom, half of Cl^- anion, one 3-obpmb ligand and half of L ligand. Each Cd atom is six-coordinated by two Cl atoms (Cl1, Cl1A), two O (O1, O2) atoms of chelating carboxylate groups from L ligand and two N (N2, N3B) atoms from two 3-obpmb ligands (Fig. 5a). The mean Cd–O, Cd–N and Cd–Cl bond lengths (2.3681(17) Å *vs* 2.3495(3) Å *vs* 2.6087(10) Å) are little longer than those of the corresponding one in $\{[Cd(BMB)(HBMB)Cl]\cdot H_2O\}_n$ (2.357(5) Å *vs* 2.332(5) Å *vs* 2.591(3) Å, HBMB = 4-benzimidazole-1-yl-benzoic acid).[24] The carboxylate groups of L ligands in **5** also display μ_1-η^1:η^1 coordination mode (Scheme 2c), which is similar to that in **3** and **4**. Cd1 atom and its own symmetry-related atoms are linked by four N atoms from two 3-obpmb ligands to afford a $[Cd_2(3\text{-obpmb})_2]$ unit (Fig. 5b). Such $[Cd_2(3\text{-obpmb})_2]$ units are linked together by two μ_2-Cl groups producing a 1D $[Cd_2Cl_2(3\text{-obpmb})_2]_n$ chain extending along *a* axis (Fig. 5b). Within the $[Cd_2Cl_2(3\text{-obpmb})_2]_n$ chain, the neighboring Cd···Cd separation is 3.740 Å. The L ligands are employed as the bridges to link the neighboring 1D $[Cd_2Cl_2(3\text{-obpmb})_2]_n$ chains generating a 2D wrinkled network extending along *ab* plane (Fig. 5c). Adjacent networks are interconnected by H-bonding interactions between O atoms of carboxylate groups and H atoms of the pyridine ring with C10 (C10–H10···O2, 3.312 Å) to afford a 3D architecture (Fig. 5d). Similar to that of in **2**, compound **5** also show a $4^{12}6^3$ topological structure (Fig. 5e).

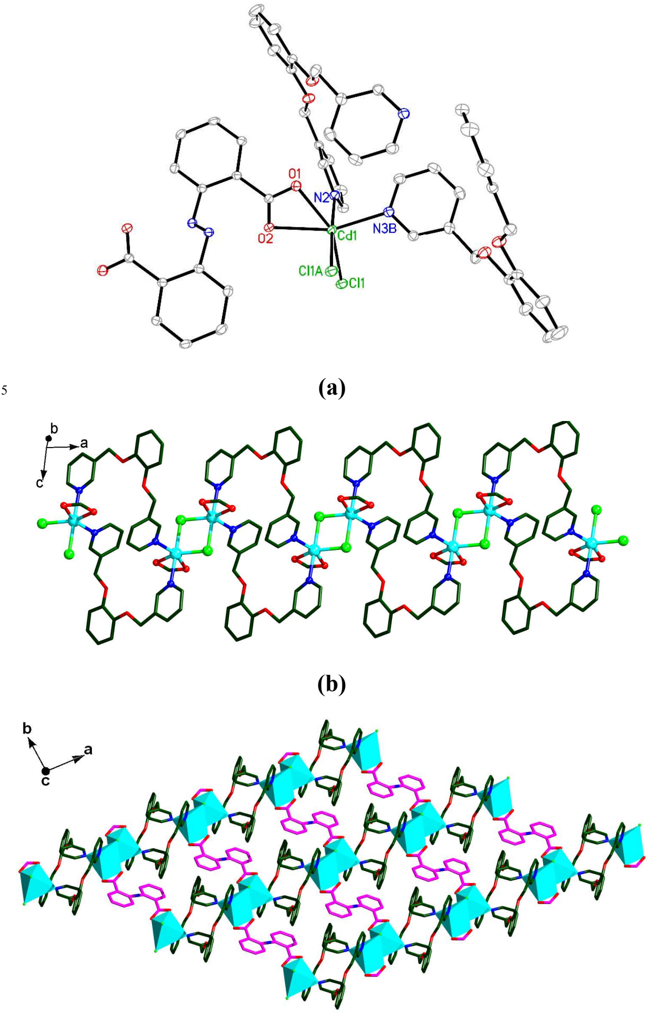

(a)

(b)

(c)

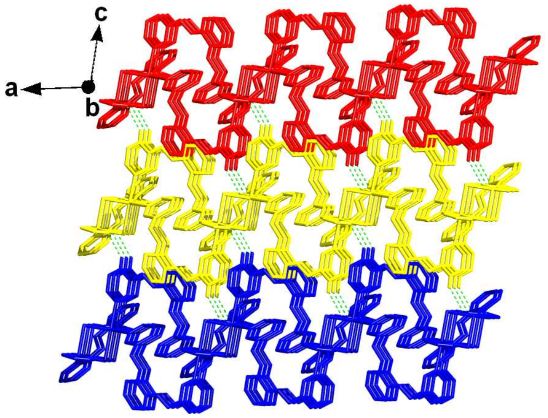

(d)

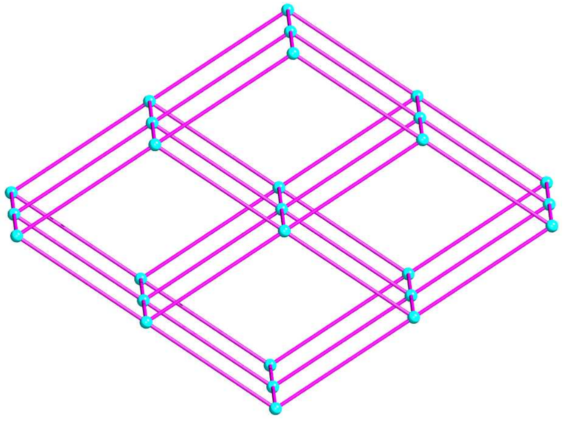

(e)

Fig. 5 (a) View of the coordination environments of Cd center in **5** with labeling schemes. Symmetry codes: (A) $-x$, $1-y$, $1-z$; (B) $1-x$, $1-y$, $1-z$. (b) View of a 1D $[Cd_2Cl_2(3\text{-obpmb})_2]_n$ chain in **5** extending along the *a* axis. (c) View of a wrinkled 2D layer in **5** extending along the *ab* plane. (d) View of a 3D hydrogen-bonded structure in **5** looking down the *b* axis. Cyan dashed lines represent the hydrogen-bonded interactions. (d) View of a *pcu* topological structure of **5**. Atom color codes: Cd, cyan polyhedrons; Cl, green; O, red; N, blue; C, dark green and pink. All H atoms except those related to H-bonding interactions are omitted for clarity.

Structural Diversity

3-pbpmb, 2-pbpmb, 4-mbpmb, 3-mbpmb and 3-obpmb are a series of N and/or O-substituted isomers of bipyridyl ligands, which are differ in the position of the N and/or O atoms at the substituted pyridyl ring as well as benzene ring. However, such a difference may significantly influence the resulting coordination frameworks. In the present study, five new Cd(II) coordination polymers have been prepared from H_2L in combination with different positional isomeric N-donor bipyridyl ligands under similar conditions. As described earlier in this article, the structures of **1**–**5** are greatly different in the following aspects. Firstly, Cd atoms in **1** and **5** are both six-coordinated and adopt the distorted octahedral coordination geometry (Fig. S6a, 6f) while these in **3** and **4** are seven-coordinated and show the bipyramidal coordination geometry (Fig. S6c, 6d, 6e). Notably, Cd atom in **2** is five-coordinated and displays the pyramidal coordination geometry (Fig. S6b). Secondly, for the isomeric linear N-donor ligands (3-pbpmb and 2-pbpmb, Scheme 1) in compounds **1** and **2**, the 3-pbpmb and 2-pbpmb exhibit *trans*-chelating modes (Schemes 3a-3b) and *trans*-bridging mode (Scheme 3c). The 3-pbpmb are connected by Cd(II) atoms affording the rhombic-like $[Cd_4(3\text{-pbpmb})_4]$ unit (Fig. 1b), while the shorter 2-pbpmb ligands are employed as bridges to link the 2D $[Cd_2L_4]_n$ networks (Fig. 2d). Thirdly, for the isomeric V-shaped N-donor ligands (4-mbpmb and 3-mbpmb, Scheme 1) in compounds **3** and **4**, which take two fashions of coordination modes and exhibit different coordination modes. In **3** and **4**, Cd(II) ions are bridged by 4-mbpmb (*cis*-chelating mode with a 120.45° of “V” in **3**, Scheme 3d) and 3-mbpmb (*trans*-bridging mode with a 100.83° of “V” in **4**, Scheme 3g) generating $[Cd_2(4\text{-mbpmb})_2]$ building unit (Fig. 3b) and 1D helical $[Cd(3\text{-mbpmb})]_n$ chain (Fig. 4c), respectively. However, only one N atom of another 4-mbpmb (*trans*-monodenate mode with a 123.40° of “V”, Scheme 3e) in **3** coordinates to Cd atom. In contrast, another 3-mbpmb in **4** takes *cis*-bridging mode with a 121.63° of “V” (Scheme 3f) and connects the helical chains resulting in the 2D network (Fig. 4d). This difference is maybe due to the smaller bending of 3-mbpmb (100.83°) as well as the *trans*-bridging mode helpful to producing the helical structure. Fourthly, comparing with 4-mbpmb in **3**, the 3-obpmb in compound **5** only takes the *trans*-chelating mode with a 57.80° of “V” (Scheme 3h) and link two Cd atoms also affording $[Cd_2(3\text{-obpmb})_2]$ unit (Fig. 5b). However, it is interesting that such $[Cd_2(3\text{-obpmb})_2]$ units are bridged by Cl^- groups instead of the N-donor ligands (4-mbpmb) obtaining 1D chain (Fig. 5b). The different coordination modes of N-donor ligands in **3**–**5** may be attributed to the different bending of N-donor ligands (120.45° for **3**, 100.83° for **4** and 57.80° for **5**). Fifthly, the dihedral angles between the benzene and pyridine rings in N-donor ligands are 89.220° (*Cg*8 and *Cg*9) and 74.683° (*Cg*12 and *Cg*11) for **3**, 89.788° (*Cg*14 and *Cg*15) and 82.081° (*Cg*14 and *Cg*16) for **4**, 77.160° (*Cg*20 and *Cg*21) for **5**, respectively, which are larger than those of in **1**–**2** (30.715°, *Cg*1 and *Cg*2; 61.167°, *Cg*4 and *Cg*5 for **1**; 46.217°, *Cg*6 and *Cg*7 for **2**] (Scheme 3, Table S2). While, the torsion angles around –O–CH$_2$– in **1**–**5** ranged from 155.9(3)° to 179.5(4)° (Table S3), which may be helpful the N-donor ligands bonding to Cd atoms. Sixthly, the carboxylate group of L ligands in **1**–**5** display μ_1-η^1:η^0 (**1**), μ_2-η^1:η^1 (**2**) and μ_1-η^1:η^1 (**1**, **3**, **4**, **5**) coordination modes (Scheme 2), respectively. Moreover, the L ligands in **1**–**4** are employed as linkers to connected Cd atoms forming 1D (**1**, **3**, **4**) and 2D (**2**) chains, while those of in **5** are only applied as building units, which may be due to the different types of N-donor ligands. Lastly, compounds **1** and **2** hold the 3D structures while compounds **3**–**5** possess 2D networks. In compounds **3** and **5**, the intermolecular hydrogen-bonding interactions between N-donor ligands (4-mbpmb, 3-obpmb) and L ligands further linked 2D networks resulting in the 3D supramolecular architectures. This difference was maybe ascribed to the bridging function of linear N-donor ligands (3-pbpmb and 2-pbpmb) in **1**–**2**, and the chelating function of V-shaped N-donor ligands (4-mbpmb, 3-mbpmb and 3-obpmb) in **3**–**5**. From the above-mentioned comparison, it is noted that the species of N-donor ligands in this study greatly affected the formation of different coordination geometries of Cd(II) atoms, the conformations and coordination modes of the L ligands and the whole structures of these compounds.

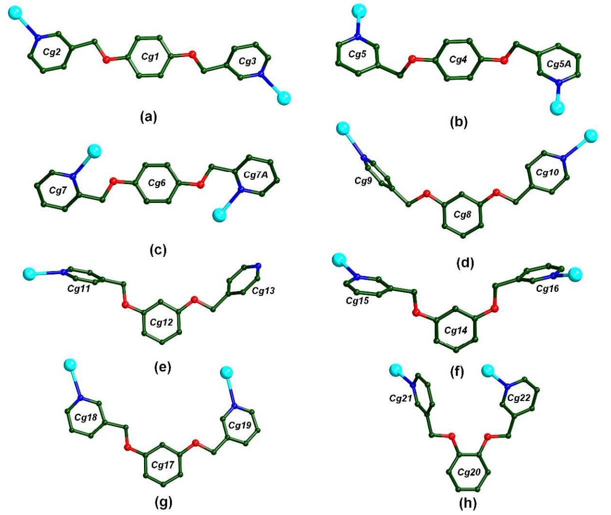

Scheme 3 Coordination modes of isomeric N-donor ligands found in compounds **1**−**5**.

Thermal properties

Thermogravimetric (TGA) experiments were carried out to study the thermal stability of **1**–**5**. As shown in Fig. S5, the TGA curves of **1**, **2** and **5** show similar profiles. Because there are no solvent molecules in the polymers, there is a plateau region ranging from 30 °C to 382 °C in **1** and 348 °C in **2**, followed by a sudden decrease in the weight, suggesting the onset of the decomposition temperature of the complexes. While for **5**, it is only stable up to 237 °C, which is much lower than that of in **1**–**2** (382 and 348 °C). This result suggests that the lattice stability of compound **5** is less than those of the others, which may be due to the 1D structure of **5** is linked by the Cl^- anions. The final residues of 16.39%, 26.17% and 24.17% for polymers **1**, **2** and **5**, respectively, are in agreement with the percentage of CdO (calculated: 15.68% for **1**, 24.38% for **2**, 22.36% for **5**), as observed in the previous studies.[6c, 23] The TGA of **3** and **4** exhibit two main steps of weight loss. The first weight losses of 2.85% in the temperature range of 89–121 °C in **3** as well as 3.29% in the temperature range of 140–181 °C in **4** show the release of lattice methanol (calculated: 3.21% for **3**) and water (calculated: 2.68% for **4**) molecules. The second step of weight losses from 417 °C corresponds to the thermal decomposition of the organic groups. The remaining weights (13.57% for **3** and 16.20% for **4**) correspond to the percentage (12.93% and 15.26%) of cadmium and oxygen components in CdO, indicating that this is the final product.

Photoluminescent Properties

Coordination polymers with d^{10} metal centers are desired candidates for fluorescence-emitting materials owing to their higher thermal stability than pure organic molecules and the ability to affect the emission wavelength of the organic materials by metal coordination.[25] Therefore, the solid-state photoluminescent spectra of compounds **1**–**5** were measured in the solid state at room temperature, as depicted in Fig. 6. Upon excitation at 330 nm leads to intense blue fluorescent emission bands at 423 nm for **1** and 435 nm for **2**, while weaker fluorescence emissions occur at 442 nm for **3**, 449 nm for **4**, as well as 469 nm for **5**, respectively. In order to understand the photoluminescent nature of **1**–**5**, the emission spectrum of the free H_2L ligand was also measured under the same conditions. However, the H_2L ligand did not show photoluminescent property in a rather wide excitation wavelength. These emission bands resemble the emission peak of free bipyridyl ligands (λ_{max} = 424 nm)[13b] and thus can be preferably ascribed to ligand-centered transitions.[26] A slightly different emission peak arises from the different coordination environments of Cd(II) centers.[27] The emission peaks of compounds **1-5** showed 12-46 nm shifts, which were similar with the previous reported d^{10} complexes.[12b, 12d, 28] Compounds **1**–**5** may be suitable as excellent candidates for the exploration of blue-fluorescent materials, since they are highly thermally stable and insoluble in common solvents.

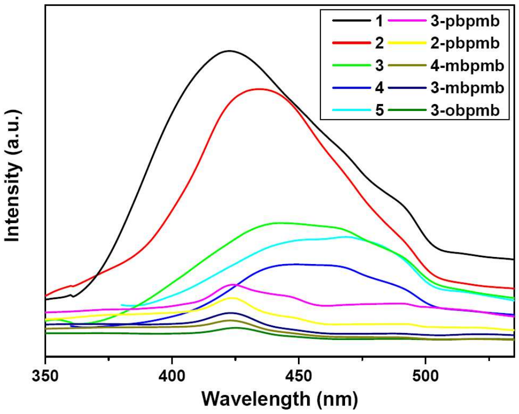

Fig. 6 Emission spectra of **1**–**5** in the solid state at ambient temperature.

Conclusions

In summary, we have presented here the synthesis, structural characterization, and properties of five cadmium(II) CPs based on flexible 2,2'-azodibenzoic acid and five positional isomeric bipyridyl ligands. Variation from the isomeric linear bipyridyl ligands (**1**–**2**) to V-shaped bipyridyl ligands (**3**–**5**), two 3D frameworks with 5-connected $4^6 6^4$ (**1**) and 6-connected $4^{12} 6^3$ (**2**) topological nets, two 3D supramolecular structures with 6^6 diamondoid network (**3**) as well as $4^{12} 6^3$ *pcu* net (**5**), and one 2D network with 6^3 topology (**4**), have been obtained. The results indicate that the differently oriented –N and/or –O atoms in the bipyridyl isomers play a significant role in the formation of the final structures. Accordingly, our present findings will further enrich the crystal engineering strategy and offer the possibility of controlling the formation of the desired network structures.

Acknowledgments

This work was supported by the National Natural Science Foundation of China (U1304210, 21401006 and 21371089) and Natural Science Projects of Department of Education of Henan Province (13A150013).

Table 2 Selected bond lengths (Å) for **1**–**5**[a]

Compound **1**					
Cd(1)–O(1)	2.244(3)	Cd(1)–N(5A)	2.345(3)	Cd(1)–O(3)	2.367(3)
Cd(1)–N(4)	2.368(3)	Cd(1)–N(3)	2.384(3)	Cd(1)–O(4)	2.472(3)
N(1)–N(1B)	1.247(6)	N(2)–N(2C)	1.245(6)		
Compound **2**					
Cd(1)–O(3A)	2.1886(16)	Cd(1)–O(1)	2.2050(16)	Cd(1)–N(3)	2.2670(17)
Cd(1)–O(2A)	2.2675(17)	Cd(1)–O(4)	2.2951(17)	N(1)–N(1B)	1.234(3)
N(2)–N(2C)	1.232(3)				
Compound **3**					
Cd(1)–O(4)	2.310(2)	Cd(1)–O(2)	2.330(2)	Cd(1)–N(5)	2.352(2)
Cd(1)–N(6A)	2.362(3)	Cd(1)–N(3)	2.392(3)	Cd(1)–O(1)	2.508(2)
Cd(1)–O(3)	2.616(3)	N(1)–N(1B)	1.242(5)	N(2)–N(2C)	1.233(5)
Compound **4**					
Cd(1)–O(5A)	2.365(2)	Cd(1)–N(6)	2.379(3)	Cd(1)–O(4)	2.379(3)
Cd(1)–N(1B)	2.384(3)	Cd(1)–N(2)	2.386(3)	Cd(1)–O(6A)	2.451(2)
Cd(1)–O(3)	2.477(2)	Cd(2)–O(13C)	2.343(2)	Cd(2)–N(7)	2.363(3)
Cd(2)–N(8C)	2.396(3)	Cd(2)–O(12)	2.415(2)	Cd(2)–N(5)	2.418(3)
Cd(2)–O(11)	2.449(2)	Cd(2)–O(14C)	2.478(3)	N(3)–N(4)	1.252(4)
N(9)–N(10)	1.240(4)	N(2)–N(2C)	1.232(3)		
Compound **5**					
Cd(1)–O(4)	2.310(2)	Cd(1)–O(2)	2.330(2)	Cd(1)–N(5)	2.352(2)
Cd(1)–N(3A)	2.311(2)	Cd(1)–O(1)	2.3296(18)	Cd(1)–N(2)	2.388(2)
Cd(1)–O(2)	2.4065(16)	Cd(1)–Cl(1)	2.5628(11)	Cd(1)–Cl(1B)	2.6546(10)
N(1)–N(1C)	1.251(4)				

[a] Symmetry codes for **1**: A: $x + 1, y, z + 1$; B: $-x + 1, -y + 1, -z + 1$; C: $-x + 1, -y, -z + 2$; Symmetry codes for **2**: A: $-x + 1, -y + 1, -z + 1$; B: $-x + 1, -y + 1, -z + 2$; C: $-x + 1, -y, -z + 1$; Symmetry codes for **3**: A: $-x + 1, -y + 2, -z + 2$; B: $-x + 1, -y + 1, -z + 2$; C: $-x, -y + 2, -z + 1$; Symmetry codes for **4**: A: $-x + 1, y - 1/2, -z + 3/2$; B: $-x + 1, y + 1/2, -z + 3/2$; C: $-x + 2, y - 1/2, -z + 3/2$; Symmetry codes for **5**: A: $-x + 1, -y + 1, -z + 1$; B: $-x, -y + 1, -z + 1$; C: $-x, -y + 2, -z + 1$.

References

1 (*a*) X. Zhao, B. Xiao, A. Fletcher, K. M. Thomas, D. Bradshaw and M. J. Rosseinsky, *Science*, 2004, **306**, 1012; (*b*) J. R. Li, J. Sculley and H. C. Zhou, *Chem. Rev.*, 2012, **112**, 869; (*c*) M. P. Suh, H. J. Park, T. K. Prasad and D. W. Lim, *Chem. Rev.*, 2012, **112**, 782. (*d*) L. J. Murray, M. Dincá and J. R. Long, *Chem. Soc. Rev.*, 2009, **38**, 1294; (*e*) Y. Yan, S. H. Yang, A. J. Blake and M. Schröder, *Acc. Chem. Res.*, 2014, **47**, 296; (*f*) R. E. Morris and P. S. Wheatley, *Angew. Chem. Int. Ed.*, 2008, **47**, 4966; (*g*) H. H. Wu, Q. H. Gong, D. H. Olson and J. Li, *Chem. Rev.*, 2012, **112**, 836; (*h*) H. Sato, W. Kosaka, R. Matsuda, A. Hori, Y. Hijikata, R. V. Belosludov, S. Sakaki, M. Takata and S. Kitagawa, *Science*, 2014, **343**, 167.

2 (*a*) L. Ma, J. M. Falkowski, C. Abney and W. Lin, *Nat. Chem.*, 2010, **2**, 838; (*b*) H. C. Zhou, J. R. Long and O. M. Yaghi, *Chem. Rev.*, 2012, **112**, 673; (*c*) O. K. Farha, A. M. Shultz, A. A. Sarjeant, S. T. Nguyen and J. T. Hupp, *J. Am. Chem. Soc.*, 2011, **133**, 5652; (*d*) M. Zhao, S. Ou and C. D. Wu, *Acc. Chem. Res.*, 2014, **47**, 1199; (*e*) P. Y. Wu, C. He, J. Wang, X. J. Peng, X. Z. Li, Y. L. An and C. Y. Duan, *J. Am. Chem. Soc.*, 2012, **134**, 14991; (*f*) Z. Q. Xu, Q. Wang, H. J. Li, W. Meng, Y. Han, H. W. Hou and Y. T. Fan, *Chem. Commun.*, 2012, **48**, 5736; (*g*) Y. Zhao, D. S. Deng, L. F. Ma, B. M. Ji and L. Y. Wang, *Chem. Commun.*, 2013, **49,** 10299.

3 (*a*) M. Maes, F. Vermoortele, L. Alaerts, S. Couck, C. E. A. Kirschhock, J. F. M. Denayer and D. E. De Vos, *J. Am. Chem. Soc.*, 2010, **132**, 15277; (*b*) D. Liu, J. P. Lang and B. F. Abarahams, *J. Am. Chem. Soc.*, 2011, **133**, 11042.

4 (*a*) P. Horcajada, C. Serre, M. Vallet-Regi, M. Sebban, F. Taulelle and G. Férey, *Angew. Chem. Int. Ed.,* 2006, **45**, 5974; (*b*) P. Horcajada, C. Serre, G. Maurin, N. A. Ramsahye, F. Balas, M. Vallet-Regí, M. Sebban, F. Taulelle and G. Férey, *J. Am. Chem. Soc.*, 2008, **130**, 6774.

5 (*a*) S. Lentijo, J. A. Miguel and P. Espinet, *Inorg. Chem.*, 2010, 49, 9169; (*b*) M. D. Allendorf, C. A. Bauer, R. K. Bhakta and R. J. T. Houk, *Chem. Soc. Rev.*, 2009, **38**, 1330; (*c*) J. Heine and K. Müller-Buschbaum, *Chem. Soc. Rev.*, 2013, **49**, 9232; (*d*) T. K. M. Lee, N .Y. Zhu and V. W.W. Yam, *J. Am. Chem. Soc.*, 2010, **132**, 17646; (*e*) Y. J. Cui, Y. F. Yue, G. D. Qian and B. L. Chen, *Chem. Rev.*, 2012, **112**, 1126; (*f*) J. Wang, C. He, P. Y. Wu, J. Wang and C. Y. Duan, *J. Am. Chem. Soc.*, 2011, **133**, 12402; (*g*) Y. Kang, F. Wang, J. Zhang and X. H. Bu, *J. Am. Chem. Soc.*, 2012, **134**, 17881; (*h*) J. Zhang, B. Zheng, T. T. Zhao, G. H. Li, Q. S. Huo and Y. L. Liu, *Cryst. Growth Des.*, 2014, **14**, 2394.

6 (*a*) M. Du, C. P. Li, C. S. Liu and S. M. Fang, *Coord. Chem. Rev.*, 2013, **257**, 128; (*b*) Z. J. Yao and G. X. Jin, *Coord. Chem. Rev.*, 2013, **257**, 2522; (*c*) B. Xu, J. Xie, H. M. Hu, X. L. Yang, F. X. Dong, M. L. Yang and G. L. Xue, *Cryst. Growth Des.*, 2014, **14**, 1629; (*d*) M. Zhu, Z. M. Hao, X. Z. Song, X. Meng, S. N. Zhao, S. Y. Song and H. J. Zhang, *Chem. Commun.*, 2014, **50**, 1912; (*e*) L.

H. Cao, Y. L. Wei, Y. Yang, H. Xu, S. Q. Zang, H. W. Hou and T. C. W. Mak, *Cryst. Growth Des.,* 2014, **14**, 1827.

7 (*a*) M. Li, D. Li, M. O'Keeffe and O. M. Yaghi, *Chem. Rev.,* 2014, **114**, 1343; (*b*) W. Zhang and R. G. Xiong, *Chem. Rev.,* 2012, **112**, 1163; (*c*) C. R. Murdock, B. C. Hughes, Z. Lu and D. M. Jenkins, *Coord. Chem. Rev.,* 2014, **258**, 119; (*d*) H. Li, Y. F. Han, Y. J. Lin, Z. W. Guo and G. X. Jin, *J. Am. Chem. Soc.,* 2014, **136**, 298; (*d*) D. S. Li, Y. P. Wu, J. Zhao, J. Zhang and J. K. Lu, *Coord. Chem. Rev.,* 2014, **261**, 1.

8 (*a*) J. X. Yang, X. Zhang, J. K. Cheng, J. Zhang and Y. G. Yao, *Cryst. Growth Des.,* 2012, **12**, 333; (*b*) G. Wu, X. F. Wang, T. Okamura, W. Y. Sun and N. Ueyama, *Inorg. Chem.,* 2006, **45**, 8523; (*c*) L. S. Long, *CrystEngComm,* 2010, **12**, 1354; (*d*) Y. F. Han, X. Y. Li, L. Q. Li, C. L. Ma, Z. Shen, Y. Song and X. Z. You, *Inorg. Chem.,* 2010, **49**, 10781; (*e*) M. Hu, A. A. Belik, M. Imura and Y. Yamauchi, *J. Am. Chem. Soc.,* 2013, **135**, 384; (*f*) D. Sun, N. Zhang, R. B. Huang and L. S. Zheng, *Cryst. Growth Des.,* 2010, **10**, 3699.

9 (*a*) L. Cui, G. P. Yang, W. P. Wu, H. H. Miao, Q. Z. Shi and Y. Y. Wang, *Dalton Trans.,* 2014, **43**, 5823; (*b*) G. Mukherjee and K. Biradha, *Cryst. Growth Des.,* 2014, **14**, 419; (*c*) L. L. Han, X. Y. Zhang, J. S. Chen, Z. H. Li, D. F. Sun, X. P. Wang and D. Sun, *Cryst. Growth Des.,* 2014, **14**, 2230; (*d*) C. Li, D. S. Li, J. Zhao, Y. Q. Mou, K. Zou, S. Z. Xiao and M. Du, *CrystEngComm,* 2011, **13**, 6601; (*e*) Z. M. Zhang, L. Y. Pan, W. Q. Lin, J. D. Leng, F. S. Guo, Y. C. Chen, J. L. Liu and M. L. Tong, *Chem. Commun.* 2013, **49**, 8081.

10 (*a*) G. J. Xu, Y .H. Zhao, K. Z. Shao, Y. Q. Lan, X. L. Wang, Z. M. Su and L. K. Yan, *CrystEngComm*, 2009, **11**, 1842; (*b*) J. X. Yang, Y. Y. Qin, J. K. Cheng and Y. G. Yao, *Cryst. Growth Des.*, 2014, **14**, 1047; (*c*) B. Xu, Z. J. Lin, L. W. Han and R. Cao, *CrystEngComm*, 2011, **13**, 440; (*d*) S. Sengupta, S. Ganguly, A. Goswami, P. K. Sukul and R. Mondal, *CrystEngComm*, 2013, **15**, 8353; (*e*) Y. L. Gai, F. L. Jiang, K. C. Xiong, L. Chen, D. Q. Yuan, L. J. Zhang, K. Zhou and M. C. Hong, *Cryst. Growth Des.,* 2012, **12**, 2079.

11 (*a*) S. Sen, S. Neogi, A. Aijaz, Q. Xu and P. K. Bharadwaj, *Dalton Trans.*, 2014, **43**, 6100; (*b*) C. L. Zhang, M. D. Zhang, L. Qin and H. G. Zheng, *Cryst. Growth Des.*, 2014, **14**, 491; (*c*) L. M. Fan, X. T. Zhang, Z. Sun, W. Zhang, Y. S. Ding, W. L. Fan, L. M. Sun, X. Zhao and H. Lei, *Cryst. Growth Des.,* 2013, **13**, 2462; (*d*) F. L. Hu, W. Wu, P. Liang, Y. Q. Gu, L. G. Zhu, H. Wei and J. P. Lang, *Cryst. Growth Des.*, 2013, **13**, 5050; (*e*) J. Zhou, L. Du, Y. F. Qiao, Y. Hu, B. Li, L. Li, X. Y. Wang, J. Yang, M. J. Xie and Q. H. Zhao, *Cryst. Growth Des.,* 2014, **14**, 1175; (*f*) S. Parshamoni, S. Sanda, H. S. Jena, K. Tomar and S. Konar, *Cryst. Growth Des.,* 2014, **14**, 2022.

12 (*a*) F. P. Huang, J. L. Tian, W. Gu, X. Liu, S. P. Yan, D. Z. Liao, and P. Cheng, *Cryst. Growth Des.*, 2010, **10**, 1145; (*b*) M. Du, X. J. Jiang and X. J. Zhao, *Inorg. Chem.,* 2007, **46**, 3984; (*c*) F. P. Huang, J. L. Tian, G. J. Chen, D. D. Li, W. Gu, X. Liu, S. P. Yan, D. Z. Liao and P. Cheng, *CrystEngComm,* 2010, **12**, 1269; (*d*) T. Liu, S. N. Wang, J. Lu, J. M. Dou, M. J. Niu, D. C. Li and J. F. Bai, *CrystEngComm,* 2013, **15**, 5476; (e) N. Y. Li, Y. Ge, T. Wang, S. J. Wang, X. Y. Ji and D. Liu, *CrystEngComm,* 2014, **16**, 2168.

13 (*a*) L. J. Li, C. Qin, X. L.Wang, S. Wang, L. Zhao, G. S. Yang, H. N. Wang, G. Yuan, K. Z. Shao and Z. M. Su, *CrystEngComm*, 2012, **14**, 124; (*b*) Y. Liu, P. F. Yan, Y. H. Yu, G. F. Hou, J. S. Gao and J. Y. Lu, *Cryst. Growth Des.*, 2010, **10**, 1559; (*c*) Y. Liu, Y. H. Yu, Y. F. Liu, G. F. Hou, X. D. Wang, B. Wen and J. S. Gao, *Z. Anorg. Allg. Chem.*, 2013, **639**, 193.

14 (*a*) M. Oh, C. L. Stern and Mirkin, C. A. *Inorg. Chem.*, 2005, **44**, 2647; (*b*) C. M. Hartshorn and P. J. Steel, *J. Chem. Soc. Dalton Trans.*, 1998, 3927; (*c*) P. J. Steel and C. M. Fitchett, *Aust. J. Chem.* 2013, **66**, 443.

15 (*a*) H. W. Hou, Y. T. Fan, L. P. Zhang, C. X. Du and Y. Zhu, *Inorg. Chem. Commun.*, 2001, **4**, 168; (*b*) X. Li, W. J. Zhao, Y. Zhang, Y. Zhang, J. T. Tan, Y. L. Lu, X. Feng and X. W. Yang, *Z. Anorg. Allg. Chem.*, 2012, **638**, 785.

16 (*a*) J. Xiao, C. X. Chen, Q. K. Liu, J. P. Ma and Y. B. Dong, *Cryst. Growth Des.*, 2011, **11**, 5696; (b) L. P. Zhang, C. K. Lam, H. B. Song and T. C. W. Mak, *Polyhedron,* 2004, **23**, 2413.

17 (*a*) G. M. Sheldrick, *SHELXS-97 and SHELXL-97, Program for X-ray Crystal Structure Solution;* University of Göettingen: Germany, 1997; (b) L. L. Liu, L. Liu and J. J. Wang, *Inorg. Chim. Acta*, 2013, **397**, 75.

18 L. L. Liu, C. X. Yu, J. Sun, P. P. Meng, F. J. Ma, J. M. Du and L. F. Ma, *Dalton Trans.*, 2014, **43**, 2915.

19 L. L. Liu, C. X. Yu, Y. Zhou, J. Sun, P. P. Meng, D. Liu and R. J. Sa, *Inorg. Chem. Commun.*, 2014, **40**, 194.

20 Y. Yang, P.Du, J. F. Ma, W. Q. Kan, B. Liu and J. Yang, *Cryst. Growth Des.,* 2011, **11**, 5540.

21 A. F. Wells, *Three-Dimensional Nets and Polyhedra*; Wiley-Interscience: New York, 1977.

22 (*a*) T. Allman, R. C. Goel, N. K. Jha and A. L. Beauchamp, *Inorg. Chem.,* 1984, **23**, 914; (*b*) S. L. Li and T. C. W. Mak, *J. Chem. Soc. Dalton Trans.,* 1995, 1519.

23 D. Niu, J. Yang, J. Guo, W. Q. Kan, S. Y. Song, P. Du and J. F. Ma, *Cryst. Growth Des.,* 2012, **12**, 2397.

24 R. Mishra, M. Ahmad and M. R. Tripathi, *Polyhedron,* 2013, **50**, 22.

25 (*a*) F. P. Huang, Z. M. Yang, P. F. Yao, Q. Yu, J. L. Tian, H. D. Bian, S. P. Yan, D. Z. Liao and P. Cheng, *CrystEngComm,* 2013, **15**, 2657; (b) G. Z. Liu, S. H. Li and L. Y. Wang, *CrystEngComm,* 2012, **14**, 880.

26 Z. R. Pan, Y. Song, Y. Jiao, Z. J. Fang, Y. Z. Li and H. G. Zheng, *Inorg. Chem.,* 2008, **47**, 5162.

27 J. Tao, M. L. Tong, J. X. Shi, X. M. Chen and S. W. Ng, *Chem. Commun.,* 2000, 2043.

28 (*a*) L. F. Ma, X. Q. Li, Q. L. Meng, L. Y. Wang, M. Du and H. W. Hou, *Cryst. Growth Des.,* 2011, **11**, 175; (*b*) D. S. Chen, L. B. Sun, Z. Q. Liang, K. Z. Shao, C. G. Wang, Z. M. Su and H. Z. Xing, *Cryst. Growth Des.,* 2013, **13**, 4092.

Graphic Contents Entry

Solvothermal reactions of $Cd(OAc)_2 \cdot 2H_2O$ with 2,2'-azodibenzoic acid and five positional isomeric N-donor bipyridyl benzene ligands in $MeOH/H_2O$ at 170 °C gave rise to five coordination polymers Complexes **1–5** are characterized by elemental analysis, IR, powder X-ray diffraction, and single-crystal X-ray diffraction.

Figure for Graphic Contents Entry